Log-Rolling Micelles in Sheared Amphiphilic Thin Films

Gaurav Arya and Athanassios Z. Panagiotopoulos

Department of Chemical Engineering, Princeton University, Princeton, New Jersey 08544, USA

(Received 20 April 2005; published 28 October 2005)

Using molecular dynamics simulations, we show that sheared solutions of cylindrical micelle-forming amphiphiles behave very differently under extreme confinement as compared to the bulk. When confined to ultrathin films, the self-assembled cylindrical micelles roll along the shearing direction and align parallel to each other with their axes along the vorticity direction, as opposed to aligning parallel to the shearing direction in the bulk. It is shown that this new ''log-rolling'' phase arises due to a strong coupling between the rotational degree of freedom of the micelles and the steady sliding motion of the confining surfaces. We examine the microscopic mechanism of the log-rolling phenomenon and also discuss its dependence on the segregation strength and length of the amphiphile, the shear rate, and the film thickness.

DOI: 10.1103/PhysRevLett.95.188301 PACS numbers: 82.70.Uv, 83.80.Qr, 83.80.Uv

It is well-known that upon shearing, highly elongated objects suspended in a bulk fluid tend to align with their longest axis pointing in the direction of flow, which minimizes the drag resistance and torque they experience. An obvious manifestation of this phenomenon is in the rheology of polymers and wormlike micelles during flow processing [1,2]. In the past few decades, the concept of shearing materials has emerged as a powerful strategy for aligning self-assembled block copolymer (BC) microphases in the direction of shear and obtaining long-range orientational order; annealing under static conditions only results in local order due to extremely slow coarsening kinetics [3,4]. There now exist numerous studies which have examined shear-induced alignment of cylindrical, lamellar, and spherical BC microphases in the bulk, as reviewed in Ref. [5].

Recently, BC ultrathin films have been recognized as excellent templates for producing ordered nanopatterns on surfaces [6]. Again, the shearing strategy has been proposed as a possible means to improving the alignment of both cylindrical and spherical microphases within the films. Surprisingly, only a few studies have examined the effect of shear on BC microphases present within such ultrathin films, where confinement-induced effects are bound to become prominent. One particular study that did examine shearing of a thin film consisting of a monolayer of flat-lying BC cylindrical microphases [7] showed that confinement did not affect the final orientation of the BC cylinders, as they were found to align parallel to the shearing direction, as in the bulk.

In this Letter, we discuss the emergence of a novel ''log-rolling'' cylindrical phase upon shearing ultrathin films of short amphiphilic molecules in solution, using molecular dynamics simulations. Upon shearing, the cylinders do *not* align parallel to the shearing direction, but rather roll about their axis, yielding cylinders aligned perpendicular to the shearing direction. We illustrate the microscopic mechanism of the log-rolling phenomenon, and also discuss its extent and dependence upon the length, segregation strength, and concentration of the amphiphilic species, and the film thickness.

Our model system, mimicking the experimental setup [7], consists of a monolayer of self-assembled cylindrical microphases (micelles) present in a selective solvent and confined between two walls (see Fig. 1). The amphiphiles are modeled as a bead-spring chain with four beads assigned to each of the solvophilic (H) and solvophobic (T) blocks. The amphiphiles hence closely resemble surfactants or very short diblock copolymers. This model [8] has previously been used in modeling shear-induced ordering of spherical micelles [9]. Briefly, the beads with mass m are connected to each other via finitely extensible nonlinear elastic springs, and all bead pairs except the T-T pairs interact with each other through a short-range repulsive Weeks-Chandler-Anderson potential with parameters ϵ and σ representing the energy and length scales, respectively. All quantities presented here are expressed in units of m, ϵ, and σ. To promote microphase separation, the T beads interact with each other through a potential which is a combination of a repulsive Weeks-Chandler-Anderson potential and a short-ranged attractive potential with a cutoff distance of 1.5σ and a well depth of $\mathcal{E}$. The confining walls are composed of a single layer of atoms arranged in a square pattern with a lattice spacing $\delta = 1.56$, where each wall atom resembles a single H bead. The solvent, selective to the micelle corona, is modeled identically to

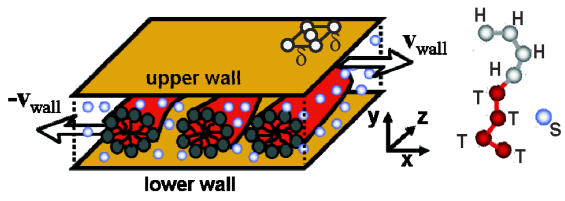

FIG. 1 (color online). Schematic of the simulation setup showing cylindrical micelles confined between two atomistic walls. Also shown is a schematic of our amphiphile model (H_4T_4) and solvent (S).

the H beads. Periodic boundary conditions are imposed in the x and z directions. Shear is imposed on the thin films by sliding the upper and lower walls at equal and opposite speeds v_{wall} in the $\pm x$ directions. The temperature is maintained constant using a profile-unbiased Nosé-Hoover thermostat [10]. In order to ensure that the temperature is being maintained correctly in our simulations, the ''kinetic'' temperature is routinely checked against the ''configurational'' temperature [11]. The equations of motion are integrated using a time step of 0.005, and the simulations are typically performed for a time $t = 10\,000$.

Figure 2 shows an approximate phase diagram for the above amphiphile solution confined to a wall separation distance $h = 10$ at an overall bead number density $\rho = (rN_a + N_s)/V = 0.5$ and temperature $k_BT = 1$. Here N_a and N_s are the total number of amphiphile and solvent molecules, respectively, r is the number of beads in an amphiphile, and V is the system volume. The diagram was obtained via analysis of micelle conformations at the end of the canonical simulation runs at varying amphiphile volume fractions $\phi = rN_a/(rN_a + N_s)$ and segregation strengths $\mathcal{E}$. Our choice of a fairly moderate overall density allows our amphiphiles to have moderately fast dynamics, since higher densities lead to extremely sluggish systems which cannot be probed with our computational resources. The parameter $\mathcal{E}$ takes the role of an inverse temperature, somewhat like the Flory-Huggins parameter χ. For $\mathcal{E} < \mathcal{E}_{\text{odt}}(\approx 1.2)$, the system becomes disordered. The focus of our simulations is within the well segregated cylindrical micelles obtained at large ϕ and $\mathcal{E}$ (see Fig. 2). This yields slightly compressed cylindrical micelles with diameter of $D \approx 11$. Our first set of simulations explore shearing of our low-density amphiphile melt at $\phi = 1$ and $\mathcal{E} = 1.6$ at different shear velocities. The lateral dimensions of our simulation box are kept fixed at $L_x = L_z = 60$ for all simulations conducted in this study.

Contrary to experimental findings [7] and our previous study [12], the fully formed micelles do not align parallel to the shearing direction. Instead, the micelles roll about their cylindrical axis, which approximately points in the flow vorticity direction. Eventually, the micelles also align in this direction, which is perpendicular to the shearing direction. Figs. 3(a)–3(f) shows the time evolution of a thin film being sheared at a shear rate of $\dot{\gamma} = 0.016$, which illustrates the microscopic mechanism of log rolling. The shear rates are computed across the micelles cores *only* using the relation $\dot{\gamma} = dv_x/dy$, where v_x is the mean velocity of amphiphiles in the shear direction. Starting from a disordered state, the amphiphiles quickly self-assemble into interconnected micelles. During this coarsening process, portions of micelles which are aligned at nonzero angles to the shearing direction begin to roll about their axis. The rolling behavior arises as a result of the direct coupling of the micelle coronas, which are composed of dangling H beads, with the torque-producing antagonistic motion of the confining surfaces. The micelles roll as intact solid objects where individual amphiphiles exhibit angular motion without any net displacements in the x direction, with exception to occasional diffusive jumps to neighboring micelles. These rolling portions of micelles gradually grow in the vorticity direction and order themselves parallel to each other by breaking off micellar linkages with other rolling micelles [see Figs. 3(c)–3(e)]. Ultimately, all intermicellar linkages break off, resulting in an almost-perfect array of micelles aligned perpendicular to the shearing direction shown in Fig. 3(f). The kinks in the micelles of Fig. 3(f) arise due to packing frustrations, which naturally disappear upon adjusting the box dimensions or the density.

Interestingly, micellar alignment resulting from their rolling motion only occurs above a critical shear rate or shear stress ($\dot{\gamma}_{\text{crit}} \approx 0.007$ for our present system). Below

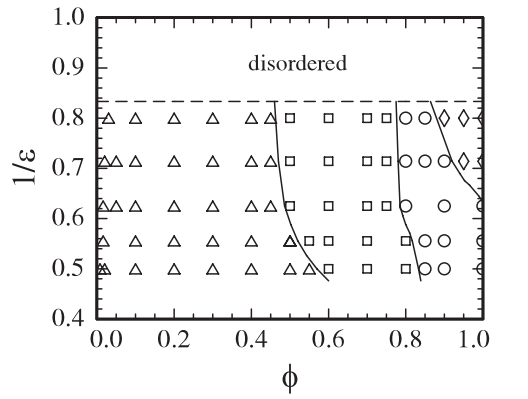

FIG. 2. Phase diagram of a confined H_4T_4 amphiphile in solution showing spherical micelles (△), mixture of spherical and cylindrical micelles (□), cylindrical micelles (○), and interconnected cylindrical micelles (◇). The solid lines represent approximate phase boundaries.

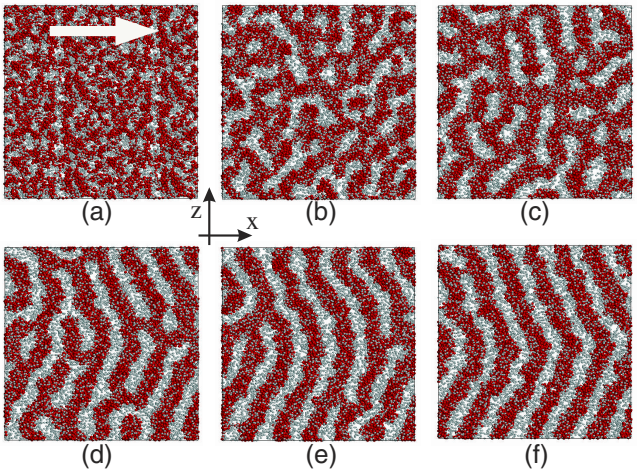

FIG. 3 (color online). Time evolution of a sheared thin film of H_4T_4 amphiphile starting from a disordered state. The snapshots have been taken from the $+y$ direction at times of $t = 0$ (a), 50 (b), 250 (c), 750 (d), 1250 (e), and 5000 (f). The arrow represents the shearing direction, while the light and dark colored spheres represent the H and T beads, respectively.

this shear rate, the micelles roll too slowly and unsteadily to generate sufficient torques to rupture intermicellar linkages, whereby the micelles remain interconnected and unaligned (as in the simulations with no imposed shear). We therefore anticipate that strongly segregated micelles would require larger shear rates to align than weakly segregated micelles. To test the above hypothesis, we conducted simulations at different segregation strengths $\mathcal{E}$. The critical shear rates at the onset of rolling and alignment are tabulated in Table I. Clearly, the more strongly the micelles are segregated, the higher the shear rates one needs to apply to align them. We have also observed that diluting the micelles with solvent has little or no effect on the magnitude of this critical shear rate (Table I). Additionally, the degree of alignment, characterized by a suitable order parameter, increases monotonically with $\dot{\gamma}$ (for $\dot{\gamma} > \dot{\gamma}_{\text{crit}}$) in a qualitatively similar manner to that observed in Ref. [12]. It would be interesting to know if the micelles continue to roll and align at very high shearing rate. Unfortunately, our simulations are unable to explore shear rates larger than 0.025. This is due to the inability of the smooth repulsive walls to transmit large stresses to the fluid; at very high shear rates, the fluid loses its "grip" with one of the walls making it to slip indefinitely over that surface [13].

To test the stability of the fully aligned log-rolling phase, we have conducted two types of simulations where (a) $\dot{\gamma}$ is suddenly reduced from its ongoing value (which is maintaining the aligned log-rolling micellar phase) to a lower value, and (b) the shearing direction is suddenly changed from its original direction. We observe that the alignment of the sheared micelles deteriorates only slightly in both the cases for long simulation runs, even when $\dot{\gamma}$ is brought to zero, or when the shear direction is changed by ± 90 deg; i.e., the micelles do not reorient in a direction perpendicular to the new shearing direction. We believe that the large energy barriers which need to be overcome in order to break and reorient fully formed and well aligned micelles are responsible for the above observations.

In order to demonstrate that log rolling is indeed confinement induced, we have performed simulations at different wall separations (film thicknesses) keeping $\phi = 0.8$ and $\rho = 0.5$ fixed. At moderate increases in the film thickness from $h = 10$, the micelles still log roll and adopt an orientation perpendicular to the shearing direction, albeit at higher shear rates due to their decreased coupling with the walls (see Table I). However, when the film thickness is increased to $h = 14$, the direct contact between the confining walls and the micelle coronas is lost and the walls are no longer able to impose a steady torque on the micelles. The micelles stop rolling and they revert back to aligning parallel to the shearing direction, as in the bulk [see Fig. 4(a)]. As the film thickness is increased, the micelles also gain more freedom to fluctuate in the direction perpendicular to the walls. This further makes log rolling particularly unstable; consider portions of a micelle coupled with the upper wall which will attempt to break away from portions of the same micelle coupled to the lower walls at other locations. The sharp peak in the cross-sectional amphiphile density ($\rho_a = rN_a/V$) profile for the log-rolling system and a relatively smoother decaying peak for the parallel-aligning system in Fig. 5 are possible signatures of a horizontal and a fluctuating micellar axis, respectively. Figure 5 also shows the velocity profiles obtained for the two scenarios at a shearing speed of $v_{\text{wall}} = 2.0$. They indicate a partitioning of the shear rate across the film thickness into a low shear rate band within the high shear viscosity region comprising the tightly bound micelle cores, and high shear rate bands within the low shear viscosity regions comprising the micelle coronas. The profiles also show significant slip at the walls due to the relatively smooth and repulsive nature of the walls [14].

Figures 4(b)–4(d) show the orientation of the micelle cores after shearing them at different film thicknesses. At $h = 19$, the films are thick enough to accommodate two micelle layers. This means that the micelles are severely

TABLE I. Dependence of critical shear rate required to produce well aligned log-rolling micelles upon amphiphile volume fraction, film thickness, and segregation strength.

ϕ	$\mathcal{E}$	h	$\dot{\gamma}_{\text{crit}}$	ϕ	$\mathcal{E}$	h	$\dot{\gamma}_{\text{crit}}$
1.0	1.6	10.0	0.007	1.0	1.6	10.0	0.005
1.0	1.8	10.0	0.012	0.9	1.6	10.0	0.004
1.0	2.0	10.0	0.014	0.8	1.6	10.0	0.005
1.0	2.2	10.0	0.016	0.8	1.6	11.0	0.009
1.0	2.5	10.0	...[a]	0.8	1.6	12.0	0.019

[a]the micelles remained unaligned at the maximum attainable shear rate $\dot{\gamma} = 0.025$.

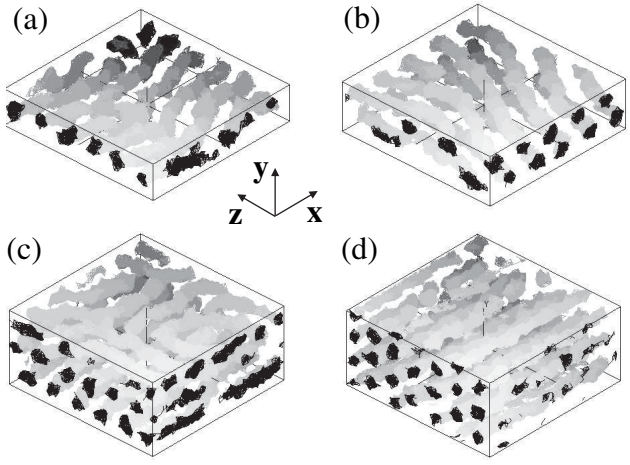

FIG. 4. Isometric view of micelle cores with $\rho = 0.5$ and $\phi = 0.8$ at different film thicknesses: (a) $h = 14$, $\dot{\gamma} = 0.004$; (b) $h = 19$, $\dot{\gamma} = 0.01$; (c) $h = 28$, $\dot{\gamma} = 0.007$; and (d) a bulk system without confining walls with $\dot{\gamma} = 0.02$. S and H beads have been omitted and the intersection of micelle cores with the facing planes of the simulation box are shaded darker for clarity.

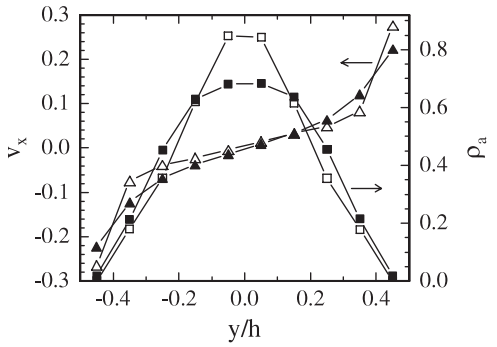

FIG. 5. Velocity (△, ▲) and amphiphile density profile (□, ■) across the normalized thickness of the sheared thin film for the log-rolling micelles of Fig. 3 at $h = 10$ and $\dot{\gamma} = 0.016$ (□, △), and the parallel-aligned micelles of Fig. 4(a) at $h = 14$ and $\dot{\gamma} = 0.019$ (■, ▲).

confined and their motion is once again strongly coupled with the motion of the confining walls. The micelles then revert back to exhibiting log-rolling motion and align perpendicular to the shearing direction. Exploring thicker films accommodating three micelle layers gives rise to an interesting scenario where the micelles sandwiched in the middle layer align parallel to the shearing direction, while micelles in the two outer layers may either align parallel to the shearing direction or log roll and align perpendicular to it. In even thicker films accommodating n micelles, the $(n - 2)$ innermost micelle layers always align parallel to the shearing direction. Interestingly, micelles in bulk systems where the confining walls have been replaced by Lees-Edwards periodic boundary conditions [15] always align parallel to the shearing direction [see Fig. 4(d)], consistent with experiments. These results confirm the confinement-driven nature of the log-rolling phenomenon.

One question that has not been addressed so far is: why do the experimental block copolymer micelles of Ref. [7] align parallel to the shearing direction and not exhibit log rolling? One possible answer to this question is that the experimental diblock polymers have molecular weights of 13.2 and 4.9 kDa for their H and T blocks, respectively. This means that the micelle coronas from neighboring micelles interpenetrate extensively with each other, which prevents the micelles from rolling. Our log-rolling micelles, on the other hand, do not show any evidence of such interpenetration. To test the above hypothesis, we have performed simulations of H_8T_4 and $H_{12}T_8$ amphiphiles which form micelles with longer and more interpenetrated coronas. In both cases, our simulations demonstrate that the micelles now become incapable of rolling and instead align parallel to the shearing direction, thus confirming our hypothesis.

Finally, we would like to comment on the applicability of our results to experimental systems. Our simulations suggest the existence of a log-rolling micellar phase when micelles are sufficiently coupled with the confining surfaces and their rotation is not hindered by the interpenetration of neighboring corona. Such a situation is likely to arise in dilute solutions of cylinder-forming surfactants or block copolymers where the micelles interact minimally with each other. In addition, the micelle monolayer would have to be adequately compressed by the shearing surfaces to the extent that the normal pressure is borne by the micelles rather than the more compressible solvent. Our simulations also indicate the onset of rolling-induced alignment at fairly high shear rates, on the order of 10^6–10^7 s^{-1} [9]). We argue that these shear rates are not that nonphysical once we normalize them with the fast time scales associated with the dynamics of our short amphiphiles. Also, we anticipate that this critical shear rate will decrease by several orders of magnitude for weakly segregated block copolymer thin films, which exhibit dynamics several orders of magnitude slower than our short model amphiphiles. In conclusion, we believe that the log-rolling micellar phase discussed in this Letter is realistic, and its existence should be measurable in experimental systems.

This work was supported by the NSF (MRSEC Program) through the Princeton Center for Complex Materials (DMR 0213706). Additional support was provided by ACS-PRF (Grant No. 38165-AC9). We also thank Paul Chaikin and Richard Register for helpful discussions.

[1] R. G. Larson, *The Structure and Rheology of Complex Fluids* (Oxford University Press, New York, 1999).
[2] M. Kröger, Phys. Rep. **390**, 453 (2004).
[3] M. C. Newstein, B. A. Garetz, N. P. Balsara, M. Y. Chang, and H. J. Dai, Macromolecules **31**, 64 (1998).
[4] C. Harrison, Z. Cheng, S. Sethuraman, D. A. Huse, P. M. Chaikin, D. A. Vega, J. M. Sebastian, R. A. Register, and D. H. Adamson, Phys. Rev. E **66**, 011706 (2002).
[5] I. W. Hamley, J. Phys. Condens. Matter **13**, R643 (2001), and references therein.
[6] M. Park, C. Harrison, P. M. Chaikin, R. A. Register, and D. H. Adamson, Science **276**, 1401 (1997).
[7] D. E. Angelescu, J. H. Waller, D. H. Adamson, P. Deshpande, S. Y. Chou, R. A. Register, and P. M. Chaikin, Adv. Mater. **16**, 1736 (2004).
[8] H. Guo and K. Kremer, J. Chem. Phys. **119**, 9308 (2003).
[9] G. Arya, J. Rottler, A. Z. Panagiotopoulos, D. J. Srolovitz, and P. M. Chaikin, Langmuir (to be published).
[10] D. J. Evans and G. P. Morriss, *Statistical Mechanics of Nonequilibrium Liquids* (Academic Press, London, 1990).
[11] B. D. Butler, O. Ayton, O. G. Jepps, and D. J. Evans, J. Chem. Phys. **109**, 6519 (1998).
[12] G. Arya and A. Z. Panagiotopoulos, Phys. Rev. E **70**, 031501 (2004).
[13] P. A. Thompson and S. M. Troian, Nature (London) **389**, 360 (1997).
[14] G. Arya, H.-C. Chang, and E. J. Maginn, Phys. Rev. Lett. **91**, 026102 (2003).
[15] A. W. Lees and S. F. Edwards, J. Phys. C **5**, 1921 (1972).